Optimal fluoroscopic viewing angles of right-sided heart structures in patients with tricuspid regurgitation based on multislice computed tomography

Tian-Yuan Xiong[1,2], MBBS, PhD; Michele Pighi[2,3], MD; Pascal Thériault-Lauzier[2], MD, PhD; Jonathan Leipsic[4], MD; Marco Spaziano[2], MSc, MD; Giuseppe Martucci[2], MD; Jean Buithieu[2], MD; Negareh Mousavi[2], MD; Thomas Pilgrim[5], MD; Fabien Praz[5], MD; Stephan Windecker[5], MD; Mao Chen[1], MD, PhD; Nicolo Piazza[2]*, MD, PhD

1. Department of Cardiology, West China Hospital, Sichuan University, Sichuan, China; 2. Department of Medicine, Division of Cardiology, McGill University Health Centre, Montreal, QC, Canada; 3. Department of Cardiology, Azienda Ospedaliera Universitaria Integrata of Verona, Verona, Italy; 4. Department of Radiology, St. Paul's Hospital, Vancouver, BC, Canada; 5. Department of Cardiology, Bern University Hospital, University of Bern, Bern, Switzerland

KEYWORDS

- imaging modalities
- MSCT
- tricuspid disease

Abstract

Aims: This study sought to analyse multislice computed tomography (MSCT) data of patients with tricuspid regurgitation and to report the variability of fluoroscopic viewing angles for several right-sided heart structures, as well as chamber views of the right heart in order to determine the optimal fluoroscopic viewing angles of six right-sided heart structures and right-heart chamber views.

Methods and results: The MSCT data of 44 patients with mild to severe tricuspid regurgitation (TR) were retrospectively analysed. For each patient, we determined the optimal fluoroscopic viewing angles of the annulus/orifice *en face* view of the tricuspid valve, atrial septum, superior vena cava (SVC), inferior vena cava (IVC), coronary sinus (CS) and pulmonary valve. In this TR patient cohort, the average fluoroscopic viewing angle for the *en face* view of the tricuspid valve annulus was LAO 54-CAUD 15; RAO 10-CAUD 66 for the SVC orifice; LAO 27-CRA 59 for the IVC orifice; RAO 28-CRA 19 for the CS orifice; RAO 33-CAUD 33 for the atrial septum and LAO 13-CAUD 52 for the pulmonary valve annulus. The average viewing angle for right-heart chamber views was LAO 55-CAUD 15 for the one-chamber view; RAO 59-CAUD 54 for the two-chamber view; RAO 27-CRA 19 for the three-chamber view and LAO 5-CRA 60 for the four-chamber view.

Conclusions: MSCT can provide patient-specific fluoroscopic viewing angles of right-sided heart structures. This information may facilitate transcatheter right-heart interventions.

*Corresponding author: Division of Cardiology, Department of Medicine, McGill University Health Centre, The Royal Victoria Hospital, 1001 Boul. Décarie, Montréal, QC H4A 3J1, Canada. E-mail: nicolopiazza@mac.com

Abbreviations

CI	confidence interval
CS	coronary sinus
IVC	inferior vena cava
MSCT	multislice computed tomography
RCA	right coronary artery
SVC	superior vena cava
TR	tricuspid regurgitation

Introduction

Fluoroscopy is a two-dimensional imaging modality that is affected by parallax[1]. Parallax error due to suboptimal fluoroscopic C-arm positions can result in apparent foreshortening or misalignment of heart structures and/or prosthetic devices[2]. Recently, there has been surging interest in transcatheter tricuspid valve interventions. Although the anatomical and functional components of the right heart have been the topic of many publications, little consideration has been given to understanding their fluoroscopic configurations[3,4]. A better knowledge of optimal fluoroscopic viewing angles of right-sided heart structures is desirable to improve preprocedural planning and reduce procedural time, radiation dose, contrast volume, and complications during transcatheter tricuspid valve interventions. Such knowledge should not be limited to a single structure but should also extend to heart chambers[5] formed by several structures in order to follow fluoroscopic guidance better and communicate within the Heart Team.

Cardiac multislice computed tomography (MSCT) can provide valuable three-dimensional (3D) geometrical data concerning the position of cardiac structures[2]. Multiplanar reconstruction of MSCT images can predict optimal fluoroscopic viewing angles for transcatheter therapies[6-8]. Our group has previously described the concepts of optimal fluoroscopic viewing angles of left-sided heart structures and their variability using MSCT[2].

The present study sought to analyse MSCT data of patients with tricuspid regurgitation and to report the variability of fluoroscopic viewing angles for several right-sided heart structures, as well as chamber views of the right heart.

Methods

In the present study, the MSCT data of 44 patients with mild to severe tricuspid regurgitation (TR) were retrospectively analysed from databases for transcatheter aortic valve replacement in two centres (McGill University Health Centre, Canada, and West China Hospital, Sichuan University, China). The severity of TR was assessed and graded by transthoracic echocardiography in accordance with practice recommendations[9]. MSCT was performed in spiral/helical acquisition mode with retrospectively electrocardiogram-gated reconstruction, with tube voltage of 100 or 120 kV and tube current according to patient size. For acquisition of the MSCT data set, 80-100 mL of contrast (370 mg iodine/mL) was injected at a rate of 4 mL/s. The image acquisition window extended from the neck to the diaphragm and image acquisition was performed in a cranio-caudal direction. MSCT data were reconstructed in 10% intervals throughout the cardiac cycle images with a slice thickness of 0.6 mm and an increment of 0.4 mm. Written informed consent was obtained from all study participants.

Fluoroscopy and MSCT share X-ray as a common image contrast mechanism; it is therefore possible to use MSCT volumetric data to simulate fluoroscopic images. Optimal viewing angles were recorded following multiplanar reconstruction using FluoroCT 3.0 (Circle Cardiovascular Imaging Inc., Calgary, AB, Canada). This software allows double oblique views from which the cranio/caudal (CRA/CAUD) and right anterior oblique/left anterior oblique (RAO/LAO) fluoroscopic angles can be derived from the oblique sagittal and oblique transverse views, respectively. Two investigators collected data independently to test reproducibility.

Optimal projection curves, which are perpendicular to the *en face* view of the structure of interest, were calculated using the following formula, embedded in the FluoroCT application[2]:

$$\emptyset = -\arctan\left[\frac{\cos(\theta - \theta_{en\ face})}{\tan \emptyset_{en\ face}}\right]$$

where $\emptyset$ is the cranio-caudal angle of the optimal projection curve at RAO/LAO angle θ, and $\emptyset_{en\ face}$ and $\theta_{en\ face}$ are, respectively, the cranio-caudal and RAO/LAO angles of the structure viewed *en face*.

Herein, we report viewing angles of six right-sided heart structures (tricuspid valve annulus, atrial septum, superior vena cava [SVC], inferior vena cava [IVC], coronary sinus [CS], pulmonary valve annulus) **(Figure 1)**. For each structure, we recorded the annulus/orifice *en face* view and its perpendicular optimal projection curve. After determining these structures, we also validated the angles of previously proposed right-heart fluoroscopic chamber views, which were defined as follows[5]:

– The one-chamber view corresponds to the short-axis view of the tricuspid annulus.

– The two-chamber view corresponds to the fluoroscopic angulation where both tricuspid valve annulus and coronary sinus are in plane.

– The three-chamber view corresponds to the fluoroscopic angulation where both tricuspid valve and pulmonary valve annuli are in plane, and the right ventricular outflow tract is elongated.

– The four-chamber view corresponds to the fluoroscopic angulation where both tricuspid valve annulus and atrial septum are in plane.

STATISTICAL ANALYSIS

Continuous variables were reported as mean±standard deviation, and categorical variables were reported as frequencies. To test for differences in means between groups with continuous variables, an unpaired Student's t-test or Mann-Whitney non-parametric test was used. For comparisons between categorical variables, the chi-squared test or Fisher's exact test was used. Viewing angles are expressed as mean with 95% confidence interval (CI) in each group taking the average value from both observers. Discrepancy between investigators was assessed by measuring the angle
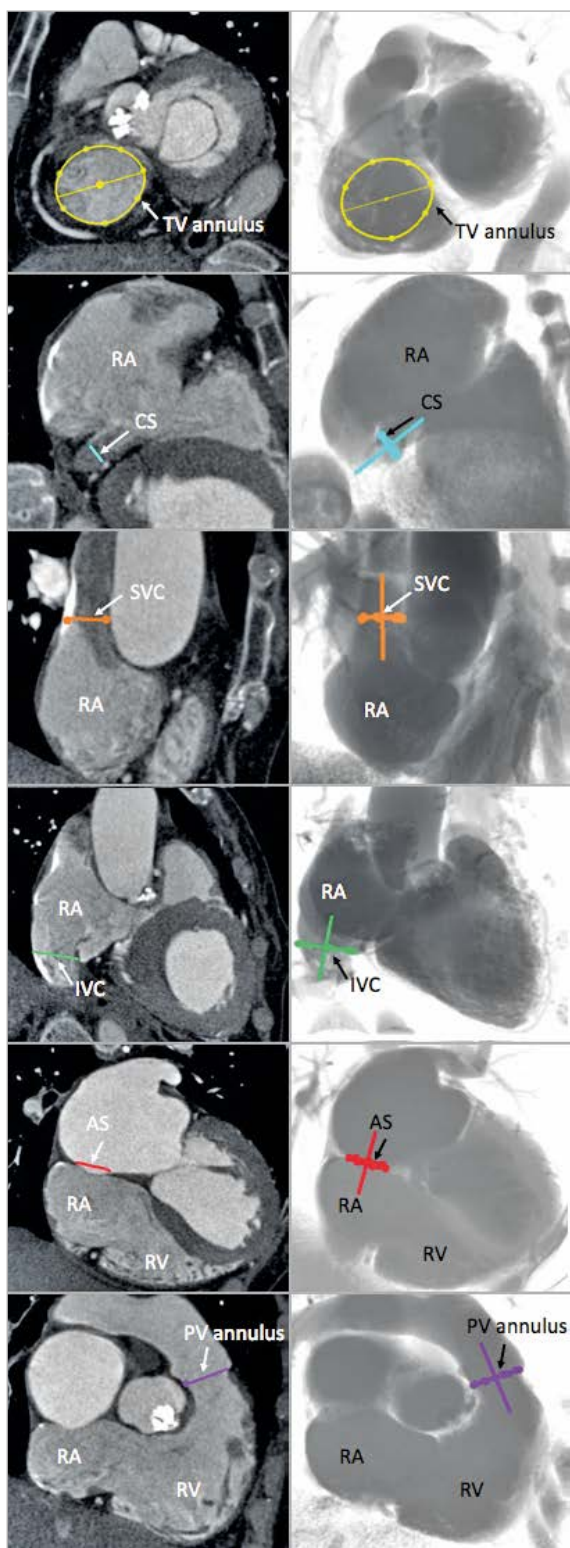
Figure 1. *Multislice computed tomography views of right-sided heart structures and corresponding fluoroscopic views. Examples of images of the six structures (AS: atrial septum, in red; CS: coronary sinus, in blue; IVC: inferior vena cava, in green; PV: pulmonary valve, in purple; SVC: superior vena cava, in orange; TV: tricuspid valve, in yellow) determined on MSCT (left column) and the simulated fluoroscopy (right column). RA: right atrium; RV: right ventricle*

between viewing planes recorded by each investigator with paired tests. The statistical analysis was performed using MATLAB Release 2013a (MathWorks, Natick, MA, USA) assuming that the directional data were distributed according to the von Mises-Fisher distribution. Statistical significance was set at two-tailed p=0.05.

Results

Table 1 shows the baseline characteristics of patients grouped as non-severe and severe TR. **Figure 2** illustrates the mean optimal projection curves and 95% CI for the tricuspid annulus, SVC orifice, IVC orifice, atrial septum, coronary sinus orifice and pulmonary valve annulus, with the optimal projection curves of every individual patient displayed.

Table 2 shows the mean fluoroscopic viewing angles of right-sided heart structures according to TR severity. The mean difference in *en face* viewing angle between severe and non-severe TR patients ranged from 3° for the SVC orifice to 10° for the pulmonary valve annulus.

Table 3 provides the average fluoroscopic viewing angles for the various chamber views.

The angles between planes of the tricuspid valve annulus vs IVC, vs SVC, vs CS, vs atrial septum and vs pulmonary valve annulus were 87±12°, 68±11°, 84±14°, 81±13° and 128±19°, respectively (for patients with severe TR vs non-severe TR they were 87±14° vs 88±11°, p=0.77; 71±11° vs 66±10°, p=0.11; 89±15° vs 79±12°, p=0.03; 86±13° vs 76±11°, p=0.01; and 125±26° vs 130±10°, p=0.41).

The inter-observer angle deviation for *en face* viewing angles ranged from 6° (95% CI: 4°-8°) to 14° (95% CI: 11°-17°) **(Table 4)**; the *en face* tricuspid annulus view had the smallest variability while the *en face* coronary sinus view had the greatest variability.

Discussion

The current study provides unique insights into the fluoroscopic angles of right-sided heart structures and chamber views. The major findings of the current study are: (i) right-sided chamber views provide the basis for fluoroscopic pattern recognition of cardiac structures; (ii) right-sided heart structures have a predictable range of optimal fluoroscopic viewing angles; and (iii) there are differences in fluoroscopic viewing angles of right-sided structures between severe and non-severe TR patients, but within 10 degrees. Although the current study provides the average viewing angles of various structures and chamber views, it should not deter the operator from obtaining patient-specific viewing angles for procedural guidance.

Transcatheter interventions involving the right heart are steadily increasing. Unlike fluoroscopic imaging of the coronary arteries or left-sided heart structures, the right heart is less familiar to operators. Given the paucity of transcatheter tricuspid valve interventions currently performed, fluoroscopic pattern recognition of right-sided heart structures is poorly understood. Although echocardiography remains essential during transcatheter tricuspid valve interventions, delivery catheters and prostheses are

Table 1. Baseline characteristics of the study population.

|	Overall cohort (n=44)	Severe TR (n=21)	Non-severe TR (n=23)	*p*-value
Age, years	77.9±8.2	77.8±10.1	77.9±7.5	0.97
Female, n (%)	29 (65.9%)	15 (71.4%)	14 (60.9%)	0.46
Body mass index, kg/m²	23.2±4.3	23.1±5.0	23.2±4.1	0.98
Hypertension, n (%)	21 (47.7%)	8 (38.1%)	13 (56.5%)	0.22
Diabetes, n (%)	11 (25.0%)	6 (28.6%)	5 (21.7%)	0.60
Coronary artery disease, n (%)	17 (38.6%)	8 (38.1%)	9 (39.1%)	0.94
Atrial fibrillation, n (%)	21 (47.7%)	10 (47.6%)	11 (47.8%)	0.99
Pacemaker, n (%)	7 (15.9%)	6 (28.6%)	1 (4.3%)	0.04
Left ventricular ejection fraction, %	48.9±15.5	50±15	49±16	0.82
More than moderate mitral regurgitation, n (%)	6 (13.6%)	4 (19.0%)	2 (8.7%)	0.40
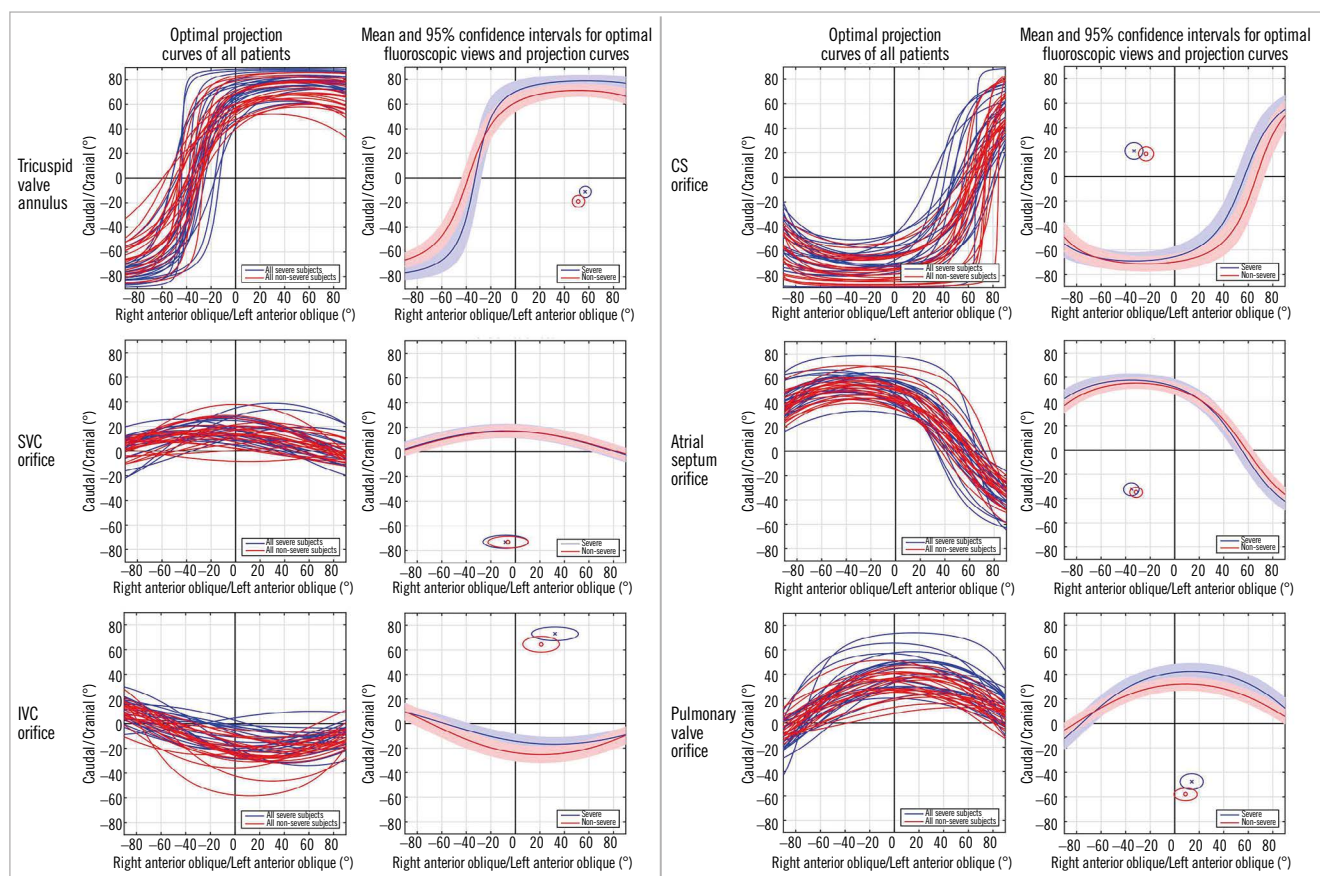
Figure 2. *Optimal projection curves for right-heart structures in patients with severe tricuspid regurgitation (blue) and non-severe tricuspid regurgitation (red). Optimal projection curves of the six structures studied from all patients are displayed in the left column. Mean and 95% confidence intervals for optimal fluoroscopic views and projection curves are displayed in the right column. The en face view of the structure (shown as circle) can be found in the quadrant without S-curve trajectory. CS: coronary sinus; IVC: inferior vena cava; SVC: superior vena cava*

inadequately visualised[10]. Moreover, the varied anatomy of the right heart, shadowing or artefacts, and other possible intracardiac leads or left-sided prostheses may all compromise the utilisation of echocardiography. On the other hand, fluoroscopy provides excellent spatial resolution of delivery catheters and prostheses with the caveat that cardiac structures are poorly visualised unless contrast injections are performed or operators have an excellent

knowledge of the relative position of right-sided cardiac structures across the fluoroscopic grid. The knowledge of optimal projection curves of right-sided structures that we summarised would thus be helpful for procedures involving these structures as we could easily navigate to their *en face* or in plane views. **Figure 3** provides the average fluoroscopic viewing angles for the right heart chambers obtained in this study. In some cases, the angulations derived

Table 2. Mean and 95% confidence intervals of optimal fluoroscopic viewing angles for right-sided structures in tricuspid regurgitation patients.

En face view	Overall cohort (n=44)	Severe TR (n=21)	Non-severe TR (n=23)	Difference between groups	*p*-value
Tricuspid valve annulus	LAO 54; CAUD 15 (LAO 51-LAO 57; CAUD 12-CAUD 18)	LAO 56; CAUD 12 (LAO 51-LAO 61; CAUD 7-CAUD 17)	LAO 51; CAUD 19 (LAO 47-LAO 56; CAUD 15-CAUD 24)	9°	0.008
SVC orifice	RAO 10; CAUD 66 (RAO 21-LAO 1; CAUD 59-CAUD 74)	RAO 9; CAUD 72 (RAO 25-LAO 7; CAUD 68-CAUD 77)	RAO 9; CAUD 75 (RAO 26-LAO 9; CAUD 71-CAUD 80)	3°	0.550
IVC orifice	LAO 27; CRA 59 (LAO 18-LAO 36; CRA 49-CRA 69)	LAO 36; CRA 74 (LAO 18-LAO 54; CRA 69-CRA 79)	LAO 24; CRA 65 (LAO 13-LAO 36; CRA 61-CRA 70)	9°	0.010
CS orifice	RAO 28; CRA 19 (RAO 24-RAO 32; CRA 16-CRA 23)	RAO 31; CRA 21 (RAO 24-RAO 37; CRA 14-CRA 27)	RAO 23; CRA 15 (RAO 18-RAO 27; CRA 11-CRA 20)	9°	0.017
Atrial septum	RAO 33; CAUD 33 (RAO 30-RAO 36; CAUD 30-CAUD 36)	RAO 36; CAUD 34 (RAO 30-RAO 43; CAUD 29-CAUD 39)	RAO 34; CAUD 37 (LAO 29-RAO 39; CAUD 33-CAUD 41)	4°	0.334
Pulmonary annulus	LAO 13; CAUD 52 (LAO 8-LAO 18; CAUD 48-CAUD 56)	LAO 13; CAUD 48 (LAO 4-LAO 23; CAUD 42-CAUD 54)	LAO 8; CAUD 58 (RAO 0-LAO 17; CAUD 53-CAUD 62)	10°	0.007

Table 3. Summary of structures in each right-heart chamber view and their average fluoroscopic viewing angles stratified by the severity of tricuspid regurgitation.

Chamber views	Overall cohort (n=44)	Severe TR (n=21)	Non-severe TR (n=23)
One-chamber view	LAO 55; CAUD 15 (LAO 52-LAO 58; CAUD 12-CAUD 18)	LAO 57; CAUD 10 (LAO 53-LAO 61; CAUD 7-CAUD 14)	LAO 53; CAUD 19 (LAO 49-LAO 57; CAUD 15-CAUD 24)
Two-chamber view	RAO 59; CAUD 54 (RAO 55-RAO 63; CAUD 51-CAUD 56)	RAO 54; CAUD 55 (RAO 48-RAO 60; CAUD 50-CAUD 59)	RAO 63; CAUD 52 (RAO 59-RAO 68; CAUD 48-CAUD 56)
Three-chamber view	RAO 27; CRA 19 (RAO 23-RAO 31; CRA 17-CRA 20)	RAO 28; CRA 19 (RAO 24-RAO 32; CRA 16-CRA 23)	RAO 26; CRA 18 (RAO 19-RAO 32; CRA 15-CRA 20)
Four-chamber view	LAO 5; CRA 60 (LAO 3-LAO 6; CRA 58-CRA 63)	LAO 5; CRA 63 (LAO 3-LAO 8; CRA 60-CRA 66)	LAO 4; CRA 58 (LAO 2-LAO 6; CRA 54-CRA 61)

Table 4. Inter-observer difference for selected views.

View	Mean difference and 95% confidence intervals, degrees		
	All patients	Severe TR	Non-severe TR
Tricuspid annulus *en face*	6 (4-8)	5 (3-8)	6 (4-7)
SVC orifice *en face*	7 (6-9)	7 (5-9)	8 (6-10)
IVC orifice *en face*	9 (7-11)	7 (5-8)	11 (9-14)
CS orifice *en face*	14 (11-17)	12 (10-14)	16 (13-19)
Atrial septum *en face*	11 (9-13)	11 (9-13)	12 (9-14)
Pulmonary annulus *en face*	8 (6-10)	7 (5-9)	8 (7-10)

from the MSCT analysis are difficult to achieve on the C-arm. Therefore, in selected cases, compromise or the use of a corresponding angle[2] may be required both to be practical and to provide useful information to the operators.

The one-chamber (or short-axis) view of the right heart (average LAO 55-CAUD 15) provides the *en face* view of the tricuspid valve and is useful to navigate catheters towards the anterior, posterior or septal leaflet of the tricuspid valve. Given that the right coronary artery (RCA) runs along the tricuspid valve annulus, the one-chamber view can provide useful information about the spatial relationship between the RCA and tricuspid annulus[11]. This view is essential when performing transcatheter annuloplasty of the tricuspid annulus (e.g., Cardioband; Edwards Lifesciences, Irvine, CA, USA) as it allows appreciating the relationship between anchors and artery[12].

The two-chamber view of the right heart (average RAO 59-CAUD 54) provides a long-axis view of the right ventricle and is similar to the two-chamber view of the left heart with respect to visualising the atrial appendage and maximally separating the papillary muscles. The two-chamber view of the right heart provides the coronary sinus and tricuspid valve both in plane, thereby mitigating parallax between these two structures and it can facilitate cannulation of the coronary sinus (versus the tricuspid annulus).
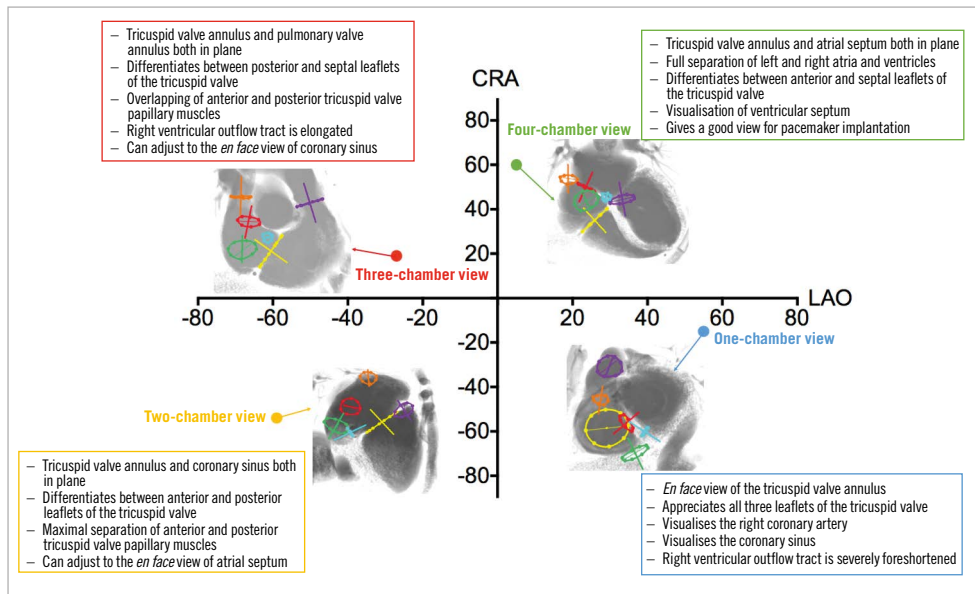
Figure 3. *Chamber views of the right heart demonstrating the relative positioning of the six structures (tricuspid valve annulus, coronary sinus, inferior vena cava, superior vena cava, atrial septum, and pulmonary valve annulus) discussed in the current study. On the fluoroscopic illustrations: tricuspid valve annulus (yellow), coronary sinus (blue), inferior vena cava (green), superior vena cava (orange), atrial septum (red), pulmonary valve annulus (purple).*

In this view, a transseptal needle will be "looking into the screen" with the atrial septum *en face*. Furthermore, the two-chamber view separates the anterior and posterior tricuspid valve leaflets, similarly to echocardiography.

The three-chamber view of the right heart (average RAO 27-CRA 19) provides a long-axis view of the right ventricle and is similar to the three-chamber view of the left heart with respect to elongating the ventricular outflow tract and overlapping papillary muscles. In the three-chamber view, the tricuspid and pulmonary valves can be found in plane; given that the right ventricular outflow tract is elongated, this view can be useful during transcatheter tricuspid or pulmonary valve replacement. Because this view separates the posterior and septal tricuspid valve leaflets, it can guide clip orientation during posterior-septal leaflet approximation. The three-chamber view has the coronary sinus *en face*, which should be discouraged during cannulation procedures of the coronary sinus.

The four-chamber view of the right heart (average LAO 5-CRA 60) can be obtained with the atrial septum and tricuspid valve annulus both in plane. The atrial and ventricular septum can be clearly visualised; this can be a useful view during ventricular septal defect closure or pacemaker positioning against the ventricular septum. The majority of tricuspid clip procedures aim to approximate the anterior and septal tricuspid valve leaflets[13]. Because the four-chamber view separates the anterior and septal tricuspid valve leaflets, it can complement echocardiography during clip orientation.

Image fusion allows the combination of multimodality imaging data sets to improve target delineation, thus it is promising for the guidance of complex interventions. With the knowledge of chamber views obtained from MSCT, fluoroscopic and echocardiography anatomy could be better understood and communicated within the Heart Team.

The tricuspid valve annulus and leaflets are currently the main target structures during transcatheter tricuspid valve interventions. Optimal projection curves provide an infinite number of angulations from which a plane of interest can be viewed perpendicularly[14]. By exploring the optimal projection curve, it is possible to visualise the plane of the tricuspid valve annulus in different chamber views and understand the relative position of right-sided heart structures. A transcatheter repair or replacement device[15-17] may require a specific chamber view that provides the annulus in plane along with other structures of interest. The optimal projection curve of the tricuspid valve annulus spans across LAO/CRA, RAO/CRA and RAO/CAUD with a characteristic steep slope in the RAO region. The region not spanned by the curve provides the *en face* view of the structure (i.e., LAO/CAUD). Pozzoli et al[18] have proposed two basic fluoroscopic projections to address the tricuspid valve anatomy. The first is the perpendicular view of the annular plane in RAO to assess the trajectory and coaxiality of the device with respect to the tricuspid annulus. The second is the *en face* view of the tricuspid valve in LAO/CAUD to navigate the catheter towards the target structure. Our results provide additional guidance to these "basic projections". The plane of the tricuspid annulus can be appreciated in the two-, three- or four-chamber view (RAO/CAUD, RAO/CRA, LAO/CRA, respectively). Based on our discussion of chamber views above, it is apparent that various right-sided heart structures can be visualised in a particular orientation with

the tricuspid valve annulus in plane. Furthermore, we provide fluoroscopic viewing angles for best appreciation of specific segments of the tricuspid valve leaflets.

Structural heart changes in severe TR have been well described and include tricuspid annular dilation and right ventricular and atrial enlargement[19,20]. Nemoto et al[21] reported that structural changes occur in proportion to TR severity. In the current study, *en face* viewing angles of right-sided heart structures varied less than expected between severe and non-severe TR (range, 3-10 degrees). Our results would suggest that fluoroscopic pattern recognition of right-sided heart structures can be extrapolated across the range of TR severity.

The inter-observer variability (within 14 degrees) was acceptable for all measured structures. This reflects solid reproducibility in defining right-sided heart structures on MSCT.

Limitations

The current study was limited by the inability to confirm acquired MSCT fluoroscopic viewing angles to actual fluoroscopic imaging during right-sided heart interventions. Some angles obtained here may be unachievable in practice, but compromise or the use of a corresponding angle (as stated in the discussion) may still be able to help. Due to image quality, it was difficult to identify the commissures accurately and therefore segments of the tricuspid valve leaflets. The current results were derived from patients with mild to severe TR; whether they can be extrapolated to patients with other pathologies is unknown.

Conclusions

The present study provides the interventional cardiologist with a general overview on the optimal fluoroscopic viewing angles and chamber views of the right heart. The average angles shown should help the operators to adapt more easily and to orient themselves to the fluoroscopy of the right heart.

Impact on daily practice

The current study provides unique insights into the fluoroscopic angles of right-sided heart structures and chamber views. The average projection angles of key structures of the right heart and the proposed chamber views should help the operators to adapt more easily and to orient themselves to the fluoroscopy of the right heart.

Conflict of interest statement

P. Thériault-Lauzier has been a consultant for Circle CVI and Cephea Valve Technology. J. Leipsic has had institutional core laboratory agreements with Edwards Lifesciences, Medtronic, Tendyne, and Neovasc, and has been a consultant for Edwards Lifesciences and Circle CVI. J. Buithieu has been a consultant for HighLife SAS, Medtronic, and Shanghai MicroPort Medical Group Co. T. Pilgrim has received research grants to the institution from Biotronik, Boston Scientific, and Edwards Lifesciences, and has received speaker fees from Biotronik and Boston Scientific. F. Praz has been a consultant for Edwards Lifesciences. S. Windecker has received research grants to the institution from Abbott, Amgen, Bayer, Boston Scientific, Biotronik, Medtronic, Edwards Lifesciences, Terumo and St. Jude Medical. M. Chen has been a consultant for Shanghai MicroPort Medical Group Co. N. Piazza has been a consultant/proctor for HighLife, Medtronic, and MicroPort, and a consultant for Cephea. The other authors have no conflicts of interest to declare.

References

1. Thériault-Lauzier P, Andalib A, Martucci G, Mylotte D, Cecere R, Lange R, Tchetche D, Modine T, van Mieghem N, Windecker S, Buithieu J, Piazza N. Fluoroscopic anatomy of left-sided heart structures for transcatheter interventions: insight from multislice computed tomography. *JACC Cardiovasc Interv.* 2014;7:947-57.

2. Spaziano M, Thériault-Lauzier P, Meti N, Vaquerizo B, Blanke P, Deli-Hussein J, Chetrit M, Galatos C, Buithieu J, Lange R, Martucci G, Leipsic J, Piazza N. Optimal fluoroscopic viewing angles of left-sided heart structures in patients with aortic stenosis and mitral regurgitation based on multislice computed tomography. *J Cardiovasc Comput Tomogr.* 2016;10:162-72.

3. Khalique OK, Hahn RT. Role of Echocardiography in Transcatheter Valvular Heart Disease Interventions. *Curr Cardiol Rep.* 2017;19:128.

4. van Rosendael PJ, Kamperidis V, Kong WK, van Rosendael AR, van der Kley F, Ajmone Marsan N, Delgado V, Bax JJ. Computed tomography for planning transcatheter tricuspid valve therapy. *Eur Heart J.* 2017;38:665-74.

5. Pighi M, Thériault-Lauzier P, Alosaimi H, Spaziano M, Martucci G, Xiong TY, Buithieu J, Ybarra LF, Afilalo J, Leipsic J, Ozden Tok O, Mousavi N, Mangiameli A, Pilgrim T, Praz F, Windecker S, Piazza N. Fluoroscopic Anatomy of Right-Sided Heart Structures for Transcatheter Interventions. *JACC Cardiovasc Interv.* 2018;11:1614-25.

6. Gurvitch R, Wood DA, Leipsic J, Tay E, Johnson M, Ye J, Nietlispach F, Wijesinghe N, Cheung A, Webb JG. Multislice computed tomography for prediction of optimal angiographic deployment projections during transcatheter aortic valve implantation. *JACC Cardiovasc Interv.* 2010;3:1157-65.

7. Binder RK, Leipsic J, Wood D, Moore T, Toggweiler S, Willson A, Gurvitch R, Freeman M, Webb JG. Prediction of optimal deployment projection for transcatheter aortic valve replacement: angiographic 3-dimensional reconstruction of the aortic root versus multidetector computed tomography. *Circ Cardiovasc Interv.* 2012;5:247-52.

8. Samim M, Stella PR, Agostoni P, Kluin J, Ramjankhan F, Budde RP, Sieswerda G, Algeri E, van Belle C, Elkalioubie A, Juthier F, Belkacemi A, Bertrand ME, Doevendans PA, Van Belle E. Automated 3D analysis of pre-procedural MDCT to predict annulus plane angulation and C-arm positioning: benefit on procedural outcome in patients referred for TAVR. *JACC Cardiovasc Imaging.* 2013;6:238-48.

9. Lancellotti P, Tribouilloy C, Hagendorff A, Popescu BA, Edvardsen T, Pierard LA, Badano L, Zamorano JL; Scientific Document Committee of the European Association of Cardiovascular Imaging. Recommendations for the echocardiographic assessment of native valvular regurgitation: an executive summary from the European Association of Cardiovascular Imaging. *Eur Heart J Cardiovasc Imaging.* 2013;14:611-44.

10. Murray CSG, Salama AY, Akdogan RE, Harb S, Nahar T, Nanda NC. Assessment of tricuspid valve by two- and three-dimensional echocardiography with special reference to percutaneous repair and prosthetic valve implantation procedures. *Echocardiography.* 2018;35:1419-38.

11. Diez-Villanueva P, Gutiérrez-Ibañes E, Cuerpo-Caballero GP, Sanz-Ruiz R, Abeytua M, Soriano J, Sarnago F, Elizaga J, Gonzalez-Pinto A, Fernandez-Aviles F. Direct injury to right coronary artery in patients undergoing tricuspid annuloplasty. *Ann Thorac Surg.* 2014;97:1300-5.

12. Stephan von Bardeleben R, Tamm A, Emrich T, Münzel T, Schulz E. Percutaneous transvenous direct annuloplasty of a human tricuspid valve using the Valtech Cardioband. *Eur Heart J.* 2017;38:690.

13. Lurz P, Besler C, Noack T, Forner AF, Bevilacqua C, Seeburger J, Rommel KP, Blazek S, Hartung P, Zimmer M, Mohr F, Schuler G, Linke A, Ender J, Thiele H. Transcatheter treatment of tricuspid regurgitation using edge-to-edge repair: procedural results, clinical implications and predictors of success. *EuroIntervention.* 2018;14:e290-7.

14. Piazza N, Mylotte D, Theriault Lauzier P. Fluoroscopic "heart chamber" anatomy - the case for imaging modality-independent terminology. *EuroIntervention.* 2016;12:Y9-15.

15. Latib A, Agricola E, Pozzoli A, Denti P, Taramasso M, Spagnolo P, Juliard JM, Brochet E, Ou P, Enriquez-Sarano M, Grigioni F, Alfieri O, Vahanian A, Colombo A, Maisano F. First-in-Man Implantation of a Tricuspid Annular Remodeling Device for Functional Tricuspid Regurgitation. *JACC Cardiovasc Interv.* 2015;8:e211-4.

16. Laule M, Stangl V, Sanad W, Lembcke A, Baumann G, Stangl K. Percutaneous transfemoral management of severe secondary tricuspid regurgitation with Edwards Sapien XT bioprosthesis: first-in-man experience. *J Am Coll Cardiol.* 2013;61:1929-31.

17. Perlman G, Praz F, Puri R, Ofek H, Ye J, Philippon F, Carrel T, Pibarot P, Attinger A, Htun NM, Dvir D, Moss R, Campelo-Parada F, Bédard E, Reineke D, Moschovitis A, Lauck S, Blanke P, Leipsic J, Windecker S, Rodés-Cabau J, Webb J. Transcatheter Tricuspid Valve Repair With a New Transcatheter Coaptation System for the Treatment of Severe Tricuspid Regurgitation: 1-Year Clinical and Echocardiographic Results. *JACC Cardiovasc Interv.* 2017;10:1994-2003.

18. Pozzoli A, Maisano F, Kuwata S, Guidotti A, Plass A, Zuber M, Russo M, Nietlispach F, Taramasso M. Fluoroscopic anatomy of the tricuspid valve: Implications for Transcatheter procedures. *Int J Cardiol.* 2017;244:119-20.

19. Kim HK, Kim YJ, Park JS, Kim KH, Kim KB, Ahn H, Sohn DW, Oh BH, Park YB, Choi YS. Determinants of the severity of functional tricuspid regurgitation. *Am J Cardiol.* 2006;98:236-42.

20. Fukuda S, Gillinov AM, Song JM, Daimon M, Kongsaerepong V, Thomas JD, Shiota T. Echocardiographic insights into atrial and ventricular mechanisms of functional tricuspid regurgitation. *Am Heart J.* 2006;152:1208-14.

21. Nemoto N, Lesser JR, Pedersen WR, Sorajja P, Spinner E, Garberich RF, Vock DM, Schwartz RS. Pathogenic structural heart changes in early tricuspid regurgitation. *J Thorac Cardiovasc Surg.* 2015;150:323-30.